AAS 06-045

NAVIGATION PERFORMANCE IN HIGH EARTH ORBITS USING NAVIGATOR GPS RECEIVER

Bill Bamford, Emergent Space Technologies
Bo Naasz, NASA Goddard Space Flight Center
Mike Moreau, NASA Goddard Space Flight Center

29th ANNUAL AAS GUIDANCE AND CONTROL CONFERENCE

February 4-8, 2006
Breckenridge, Colorado

Sponsored by
Rocky Mountain Section

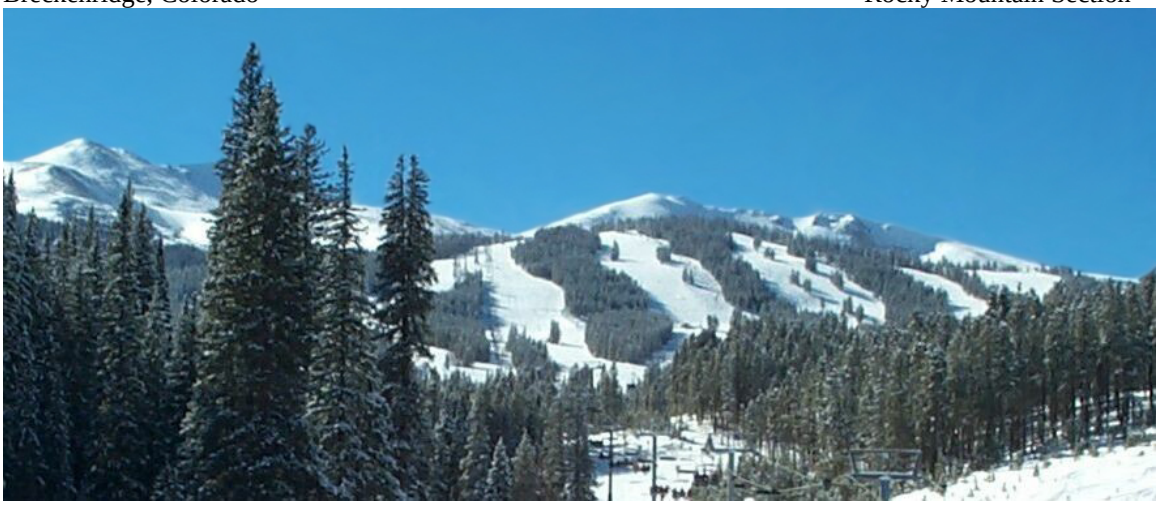

AAS Publications Office, P.O. Box 28130 - San Diego, California 92198

AAS 06-045

NAVIGATION PERFORMANCE IN HIGH EARTH ORBITS USING NAVIGATOR GPS RECEIVER

William Bamford[◊], Bo Naasz[ϒ], Michael C. Moreau[Ψ]

NASA GSFC has developed a GPS receiver that can acquire and track GPS signals with sensitivity significantly lower than conventional GPS receivers. This opens up the possibility of using GPS based navigation for missions in high altitude orbits, such as Geostationary Operational Environmental Satellites (GOES) in a geostationary orbit, and the Magnetospheric MultiScale (MMS) Mission, in highly eccentric orbits extending to 12 Earth radii and higher. Indeed much research has been performed to study the feasibility of using GPS navigation in high Earth orbits and the performance achievable. Recently, GSFC has conducted a series of hardware in-the-loop tests to assess the performance of this new GPS receiver in various high Earth orbits of interest. Tracking GPS signals to down to approximately 22-25 dB-Hz, including signals from the GPS transmitter side-lobes, steady-state navigation performance in a geostationary orbit is on the order of 10 meters. This paper presents the results of these tests, as well as sensitivity analysis to such factors as ionosphere masks, use of GPS side-lobe signals, and GPS receiver sensitivity.

INTRODUCTION

With recent advances in receiver capabilities, the Global Positioning System (GPS) is becoming an attractive alternative for satellites in geostationary or other high Earth orbits requiring improved orbit determination (OD) accuracies, reduced solution latencies, or accurate onboard state knowledge. The objective of this paper is to examine the sensitivity of GPS-based navigation performance to a number of important error sources or implementation assumptions. First, an orbit determination performance benchmark is established using the "best case" results for a geostationary user. These results utilize a GPS receiver with improved acquisition sensitivity, a high gain receiving antenna, and assume that measurements have been corrected to remove ionosphere and GPS ephemeris and clock errors. Subsequent analyses examine the sensitivity of the OD performance to factors including: receiver sensitivity and utilization of GPS side lobe signals, variations in transmitter antenna gain and transmitted power from different GPS satellites, ionosphere delays and mask settings, and GPS orbit and clock errors.

APPROACH

Two sources of GPS measurement data were utilized in this paper. Data were obtained by conducting hardware in-the-loop tests with NASA's Navigator GPS receiver[6] connected to a Spirent 4760 GPS radio frequency simulator. The GPS receiver produced filtered, real-time orbit determination solutions as well as raw GPS observables (pseudorange, Doppler, and signal to noise ratio) for post-processing. Additionally, data were generated using GSFC's Measurement Data Simulation program, or DATSIM[3]. DATSIM is a high fidelity software simulation that models the measurements produced by a GPS receiver including normal GPS error sources as well as effects due to the GPS receiver's clock. The DATSIM software makes it possible to generate many sets of data based on a wide range of simulation assumptions much more efficiently than is possible using real-time testing with a receiver.

Throughout the rest of the paper, the data recorded from the Navigator GPS receiver will be referred to as *hardware test* data, while the data generated from DATSIM will be referred to as *software simulation* data. Both sets of data were post-processed in order to investigate the sensitivity to important parameters and assumptions.

Force Model Parameters and Assumptions

A geostationary reference trajectory was generated using the Goddard Trajectory Determination System (GTDS)[1] for use as the truth orbit in both the real-time hardware test and software simulation cases. The truth model encompassed a 70x70 JGM2 gravity model, drag and solar radiation pressure models with a 12 m^2 surface area, and an 1800 kg mass.

The Navigator receiver is a new space-borne GPS receiver that is optimized for fast signal acquisition and weak signal tracking. The fast acquisition capabilities provide exceptional time to first fix performance (TTFF) with no a-priori receiver state or GPS almanac information. The fast acquisition capability also makes it feasible to implement extended correlation intervals, up to the full 20 ms data chipping interval, and therefore significantly reduce Navigator's acquisition threshold to between 22 and 25 dB-Hz. The increased sensitivity results in significantly better GPS observability at GEO than would be possible using a conventional GPS receiver. Navigator also utilizes a real-time implementation of GSFC's GPS Enhanced Onboard Navigation System (GEONS)[2]. GEONS processes sparsely available pseudorange measurements in a sequential filter and provides estimates of the receiver state even when traditional GPS point positioning would not be possible. High fidelity force and clock models enable accurate onboard state propagation during signal outages.

For this study, the GEONS state vector consisted of the receiver position and velocity, clock bias and clock drift, a solar radiation pressure coefficient and a drag coefficient. Though the receiver provides pseudorange, Doppler, carrier-phase, and signal to noise measurements, only the pseudoranges were processed in GEONS. The standard deviations used to initialize the covariance were set to 1000 meters for the position

components, 2.3 m/s for the velocity, $1x10^9$ m for the clock bias, and 3.2 m/s for the clock drift. The solar radiation pressure covariance was initialized with a 10% error. The covariance and process noise on the atmospheric drag coefficient were initialized to values that would prevent any innovation from being put into the drag, which is negligible at GEO.

Spirent GPS Simulator Settings

Table 1 lists the important Spirent GPS simulator settings used to produce the hardware test data. The GPS constellation was simulated based on a YUMA almanac file corresponding to June, 1998 (GPS week 963). The 16 channels of the RF simulator were configured to simulate the strongest 16 GPS signals present; however, many of these satellites were actually below the sensitivity threshold of the receiver at any given time.

Table 1 - Spirent Simulator Settings

Parameter	Setting	Parameter	Setting
Simulation Epoch	21 June 1998 00:00:00 UTC	**GPS Satellite Orbits**	27 Satellites from week 963 YUMA almanac
Signal Strength Offset	+15 (10 dB antenna) +9 (4 dB antenna)	**Receiver Channels**	12 Channels
GPS Ephemeris and Clock Errors	None Modeled	**Simulated Satellite Selection Metric**	16 Channels Highest Signal Strength
Measurement Noise Characteristics	Actual Noise of Receiver	**Ionosphere Errors**	None Modeled
Other Measurement Errors	None Modeled	**Receiver Clock Stability**	Actual Stability of Receiver (OCXO)
Receiver Acq. Threshold	Observed Between 23-24 dB-Hz	**Receiver Tracking Threshold**	Observed Between 21-22 dB-Hz

In order to realistically simulate GPS signals in a high altitude scenario, the GPS transmitter models and signal strength offsets must be selected with care[7]. The Spirent signal generator has the ability to accurately reproduce the power level received by the GPS receiver by carefully modeling the gain patterns of both the transmitting and receiving antennas, as well as compensating for free-space signal propagation losses. For the simulations presented here, the GPS transmitter antenna gain pattern was based on a Block II/IIA L1 reference gain pattern[12]. Two receiving antennas were modeled, a hemispherical antenna with a peak gain of 4 dB and a "high-gain" antenna with 10 dB of peak gain and an approximate 40 degree half-power beam width. For the high gain receiver antenna, the global signal strength offset in the Spirent simulator was set to +15 dB based on the following assumptions: +3dB for a "typical" minimum GPS signal strength of -157 dBW at the surface of the Earth (Spirent is referenced to -160 dBW), +10dB for receiving antenna peak gain, +0.5dB for atmosphere losses not applicable for space users, and +1.5 dB to offset cable losses between simulator RF output and receiver low-noise amplifier. For the 4 dB hemispherical receiver antenna, the global signal strength was set to +9 dB.

The simulated RF signals were generated without ionosphere errors, or errors in the broadcast GPS satellite and clock parameters. The effects of neglecting these error sources will be investigated using software simulated measurements.

GPS Receiver Initialization and Procedure

The Navigator GPS receiver begins from a cold start condition, with no a-priori knowledge of its position, the ephemeris of the GPS satellites, or the time. At the start of the geostationary scenario used here, all of the GPS signals present are very weak, with no signals stronger than -179 dBW (30 dB-Hz as reported by the receiver); however, the Navigator's advanced signal acquisition engine can typically acquire and track all available satellites within minutes. In spite of the poor instantaneous geometry typically available at GEO, the presence of four satellites simultaneously in view enables the receiver to generate a point solution with sufficient precision to initialize the GEONS filter with an estimate of position, velocity, clock offset, and clock drift. For this study, the GEONS filter initialization occurs as soon as a Navigator point solution becomes available. The Navigator then provides the filter with pseudorange measurements every 5-10 seconds. The Navigator point solution is output every second through a high speed data acquisition card, and the GEONS state estimates, covariance, and measurement residuals are exported through a serial connection for use in data analysis and post-processing. A typical hardware test resulted in a definitive estimation span of three to four days. Orbit error statistics were then generated by differencing the GEONS state vectors against the interpolated truth trajectory states. Steady-state orbit determination errors were assessed by looking at only the last third of the data arc, or approximately 24 hours worth of data, although the filter converged to steady state within the first 24 hours (one full orbit). The pseudorange measurements are also output for post-processing, and by editing measurements from the hardware test data, it is possible to re-process the data to assess error sensitivity to acquisition threshold and availability of side lobe signals.

DATSIM Model Parameters and Assumptions

In order to investigate the sensitivity of onboard orbit determination accuracy to ionospheric delay, GPS broadcast ephemeris and clock errors, changes to the GPS transmitter antenna patterns, and variations in simulated measurement noise levels, the DATSIM software was used to generate a variety of software simulated measurement data sets. The first set of software-simulated measurement data was modeled to match the hardware test data recorded by the Navigator receiver and Spirent RF simulator. Comparisons between the software simulated and hardware test data were made to better understand the correct Spirent simulator power settings, and to calibrate the DATSIM input measurement noise to match the observed Navigator measurement noise. Subsequent software simulated data sets were generated which included modeled errors for GPS ephemeris and clock, ionosphere delays, and varying GPS satellite transmitter gain patterns. The software simulation capability provides a more efficient means to generate data because simulated data may be generated much faster than real-time. Furthermore, the DATSIM has more sophisticated models for errors such as ionosphere delays and GPS ephemeris and clock than can be easily modeled in the Spirent simulator.

DATSIM settings used to generate the software simulated data are shown in Table 2. A description of the simulations performed is given in Table 3. Note that for each software-only simulation, 10 simulations were performed with varying simulated receiver clock, simulated measurement noise, and filter initial state noise seeds.

Table 2 - DATSIM Parameter Settings

Parameter	Setting	Note
GPS ephemeris error noise	0.0, 2.0	meters, 1 sigma
Pseudorange measurement noise	0.50	meters, 1 sigma
Receive antenna gain in maximum direction	10.00	dB
Receive antenna noise temperature	290.00	K
Receive antenna system losses	-4.50	dB
Transmitter reference gain (Block IIA)	14.90	dB-Watts
Receive antenna boresight direction	nadir	
Transmit antenna beam angle mask	65.00	Deg
Receive antenna beam angle mask	180.00	Deg
Receive antenna elevation angle mask	90.00	Deg
Received C/No mask	23.00	dB-Hz
Simulation span	3	days
Receiver clock Allan variance[i] parameters:		
TCXO, h0	2.00E-19	(0.009 m2/s)
TCXO, h-2	2.00E-20	(0.03553 m2/s3)
OCXO, h0	8.00E-20	(0.0036 m2/s)
OCXO, h-2	4.00E-23	(7.106E-05 m2/s3)
Observation frequency	5	s

Table 3 - Software-only (DATSIM) Simulation Description

Case	Pseudorange Measurement Noise [m]	GPS Broadcast Ephemeris Error Included? (2m S/A- like)	Ionosphere Delay Included? (GEONS algorithm 1)	Receiver Clock Model	GPS transmit antenna [Block]
1	0.5	no	no	OCXO	IIA
2	0.5	no	no	TCXO	IIA
3	0.5	yes	no	OCXO	IIA
4	0.5	no	yes	OCXO	IIA
5	0.5	yes	yes	OCXO	IIA

[i] Clock Allan variance parameters are defined in Ref. [10]

RESULTS

Data recorded from hardware in-the loop testing of the Navigator GPS receiver was edited and reprocessed to examine sensitivity to ionosphere masks, availability of GPS side lobes, and sensitivity to initial GEONS state error. Hardware test results are summarized in Table 4. Software simulated data was used to examine effects such as sensitivity to errors in the broadcast GPS ephemeris and clock data, ionosphere delays, and variations in the GPS transmitter gain patterns. These results are summarized in Table 5. Comparisons between results from both data sets were useful to calibrate measurement noise settings in the simulated data, and to better understand differences in the fidelity of hardware versus simulated data.

Table 4 - GEO Orbital Accuracy From Hardware Test (mean +/- STD)

	3D Position Error (m)	**3D Velocity Error (cm/s)**
Hardware Test Data (Baseline)	1.344 ± 0.6639	0.010 ± 0.0057
Hardware Test Data (1000 km Ionosphere Mask)	1.370 ± 0.6790	0.010 ± 0.0060
Hardware Test Data (No Side Lobes)	3.572 ± 1.914	0.026 ± 0.0108

Table 5 – Software Simulation (DATSIM) Results

Case	mean total position error [m]	position error STD [m]	mean total velocity error [cm/s]	velocity error STD [cm/s]	pseudo-range residual STD [m]	mean total semi-major axis error [m]	semi-major axis error STD [m]
1	1.0210	0.6957	0.0142	0.0083	1.3654	1.6969	2.0653
2	1.0199	0.6952	0.0142	0.0083	3.0524	1.6959	2.0644
3	1.9030	1.0180	0.0190	0.0112	2.1230	1.7625	2.0278
4	2.1891	0.8663	0.0211	0.0091	1.5950	2.9311	1.7467
5	2.6067	1.4197	0.0251	0.0148	2.2519	3.0058	2.0050

Baseline Geostationary Orbit Determination Performance

GEONS state estimates and covariance information, which are logged in real-time by the Navigator GPS receiver during the hardware test, are plotted in Figure 1-3. Error statistics for this baseline case, the equivalent software simulation case, as well as some of the other cases evaluated are summarized in Table 4.

Receiver Sensitivity and Contribution of Side-Lobes

The Navigator receiver can acquire and track weak GPS signals typically below levels of 25 dB-Hz, thus the baseline hardware test data set includes many GPS signals radiated from the GPS transmitter side lobes. Contributions from side lobe signals can improve performance significantly by filling in gaps in main lobe coverage when no GPS

satellites are available, particularly when the receiver does not use a high quality reference oscillator. The hardware test GPS observations were post-processed to remove any measurements from GPS side lobes and re-processed in GEONS to compare estimation errors with and without side lobes. A comparison of the number of satellites available, with and without side lobes is shown in Figure 4. With no side lobe signals, the maximum predictive interval (during which no GPS satellites were visible) was approximately 100 minutes. Typical predictive intervals were 30-60 minutes. Plots of the position and velocity state errors are shown in Figure 5 and Figure 6 respectively. Error statistics are summarized in Table 4. Removal of the size lobe signals does not significantly increase the errors because, 1) the predictive intervals are relatively short, and 2) the Navigator receiver utilized a very good clock, comparable in stability to a high-quality OCXO.

The sensitivity of the errors to the acquisition/tracking sensitivity of the receiver was also investigated by post processing the hardware test data set to remove measurements with reported signal to noise below various tracking thresholds. The results of this study are depicted in Figure 7. The top pane of the figure shows the estimation error mean and standard deviation, as a function of the received power. The bottom pane of Figure 7 depicts the average number of satellites tracked at a given received power level. The top pane illustrates that estimation error decreases as receiver sensitivity improves down to a sensitivity of approximately 27 dB-Hz. Below 27 dB-Hz, estimation errors stay constant. GPS side lobes start to become available for receiver sensitivities of 30 dB-Hz and below (for the assumed transmitter antenna model). The knee in the performance curve at 27 dB-Hz roughly corresponds to having 2-3 satellites present simultaneously, with little or no periods of zero GPS availability. Increasing the number of visible satellites above these levels does not result in significantly improved performance for a GEO user. However, if the user at GEO did not use a high gain antenna, then a lower receiver sensitivity would be required to obtain the same GPS observability and resulting performance.

Receiver Antenna Comparison (High Gain vs Hemispherical)

Two different receiver antenna models were evaluated, a high gain antenna with 10 dB peak gain and positive gain only out to 38 degrees, and a hemispherical antenna that only has a 4 dB peak gain, but has positive gain out to near 75 degrees. The antenna gain patterns are plotted in Figure 8. Because most of the GPS satellites tracked are within 25 to 30 degrees of the receiving antenna boresite for the GEO user, the more directional antenna actually helps put more gain where it is most useful. Neither of these antennas is necessarily optimal for a GEO user, but both are based on existing, readily available GPS antenna designs.

A software simulation of the GPS availability was conducted for both antennas, and the number of tracked satellites was tabulated and plotted in Figure 9. Though the hemispherical antenna distributes its power over a much wider angle, the power in the critical regions for tracking side lobe signals at GEO (20-30 degrees off nadir) is too weak, netting fewer tracked satellites than with the high gain antenna. Because we are

assuming a GEO user with a nadir pointing antenna, the high gain, narrow field of view antenna is used.

Sensitivity to Initial State Error

The accuracy of the state vector used to initialize the GEONS filter in real-time can vary widely based on whether the source is a kinematic "point solution" from the receiver, or whether the initial state is derived from a "ground uploaded" state vector that has some latency associated with it. To determine the effect of initial state vector error on filter performance, a sensitivity study was conducted. In this study, the hardware test data was post-processed in GEONS, at first initialized with the same position, velocity, and clock estimates utilized in real-time. Then, each of these parameters was adjusted to determine the maximum amount of initial error the filter could tolerate before it no longer converged. The results of this study are tabulated in Table 6.

Table 6 - Initial Condition Sensitivity

Parameter	Maximum Error
Total Position Error (m)	10400 (3D Error)
Total Velocity Error (m/s)	25 (3D Error)
Total Clock Bias Error (m)	9,000,000 (~ .03 seconds)
Total Clock Drift Error (m/s)	33

It is apparent that the initial position and velocity can have a significant amount of error and still converge within a few hours. The clock initialization is slightly more sensitive. The initial clock bias needs to be resolved to within 0.03 seconds and the clock drift to 33 m/s. In a few simulations, these conditions have been violated, leaving the filter in a state that does not converge. Even though the accuracy from a point solution computed at GEO can be poor compared to conventional GPS performance due to poor geometry, the position, velocity, and clock states are more than accurate enough to initialize the GEONS filter. In the absence of a point solution, obtaining a suitably accurate initial estimate of the receiver clock bias and drift is generally the most challenging part of the initialization problem. Future work on the Navigator will focus on methods of initializing GEONS with little or no information about the receiver clock states.

Sensitivity to Ionosphere Errors or Mask Settings

In previous works, pseudorange errors due to the ionospheric delay were neglected under the assumption that they could be removed using a dual frequency implementation[4]. Moreover, it was assumed that an ionosphere mask could be employed to minimize the contribution of these signals to the estimation errors. In order to validate these assumptions, a study was done to determine the effect of masking out any signals that would pass through the atmosphere. For this study, the height of the ionosphere was modeled as 1,000 Km, and the GEONS filter was configured to ignore all measurements that passed within this distance of the Earth's limb.

Table 4 lists the 3D estimation errors with and without the ionosphere mask. It is readily apparent that the application of this Height of Ray Path (HORP) editing technique has very little effect on the overall precision of the solution. The implication is that on the basis of providing ionosphere corrections, a dual frequency GPS receiver does not provide significant benefit. It was determined that the application of the mask affected less than 2% of the pseudorange measurements.

Sensitivity to GPS Ephemeris and Clock Errors

Another important source of error in a GPS onboard navigation system is the error in the broadcast ephemeris message. Previous studies have ignored GPS ephemeris and clock errors based on the assumption that these were likely not the dominate error sources at GEO, and furthermore because techniques are available whereby real-time corrections to GPS ephemeris and clock information can be utilized onboard[4]. Again, to validate some of these earlier assumptions, a study was conducted to assess the contribution of GPS ephemeris and clock errors for the geostationary user.

As-broadcast user range errors, which include errors in the broadcast GPS ephemeris and clock parameters, typically vary between 1 to 4 meters across the different GPS satellites[11]. The Spirent GPS signal simulator does not provide an easy method for modeling these errors. To simulate broadcast ephemeris errors in DATSIM, the program's Selective Availability (SA) model was used, with a noise standard deviation (1 sigma) of 2.0 meters, which, based on experience, yields ranging errors consistent in magnitude with the actual GPS ephemeris and clock errors. This model is based on the LEAR 4 model described in Ref. [9]. The addition of GPS broadcast ephemeris errors results in an increase in total position error of about 0.4 to 1.3 meters, a 1.1 to 1.8 meter increase in semi-major axis error, and an almost negligible effect (0.005 cm/s) on total velocity error.

Measurement Noise

In order to characterize the pseudorange measurement noise for the Navigator receiver at GEO, the GEONS filter residuals were studied for both strong and weak satellite signals. The GEONS measurement residuals were compared between the hardware test data and simulated data sets for various simulated measurement noise settings in an attempt to perform a first order assessment of the measurement noise from the Navigator receiver for very weak GPS signals. Only the steady state measurement residuals were used. The results of this investigation were used to scale the appropriate measurement noise for the simulated data utilized in the other studies conducted for this paper.

Figure 10 is an example of the variation in measurement noise as a function of the signal to noise ratio that was observed in the hardware test data from the navigator receiver. Measurement noise for signals below 30 dB-Hz was at a level of several meters, but was much smaller for the strongest signals. It is important to note that the

addition of weaker side lobe signals improves the number of satellites available and decreases outages, but it also introduces poorer-quality measurements into the solution.

Sensitivity to Changes in GPS Transmitter Antenna

The results presented in this paper are based on the GPS transmitter gain pattern for a Block IIA satellite[12]. The current GPS constellation actually contains three different "blocks" of GPS satellites with drastically different gain patterns, particularly in the side lobe regions. Furthermore, the model used here does not account for significant variations in transmitter gain as a function of azimuthal cut of the antenna selected.

Although data from the Block IIR and IIR-M satellites has been examined extensively by NASA GSFC, these data are considered proprietary and not yet in the public domain, so specific results are not included in this paper. Some GPS satellites actually have stronger side lobe signals than modeled for the Block IIA satellites, and some satellites have side lobe signals that are significantly suppressed. Nevertheless, the results presented in this paper, which assume a full GPS constellation using the same Block IIA antenna model on every satellite, are believed to be consistent with the actual performance provided by the current mix of satellites in the GPS constellation.

SUMMARY

This paper has presented an assessment of the navigation performance possible for a geostationary GPS user with the Navigator GPS receiver. Comparisons were made between data recorded from a GPS receiver in a hardware in-the-loop test and measurement data that was simulated in software. The sensitivity of the navigation errors to ionosphere masks, receiver sensitivity, and GPS ephemeris and clock errors was examined. These results are catalogued in Figure 11. Results indicate that utilizing a receiver with a sensitivity of 25 dB-Hz or less and a stable reference oscillator, steady state position accuracies below ten meters are achievable. Side lobe signals contributed significantly to the number of GPS satellites available, but even when side lobe signals were excluded, navigation performance did not degrade significantly.

REFERENCES

1. Computer Sciences Corporation, *Goddard Trajectory Determination System (GTDS) Mathematical Theory*, Revision 1, Long, A.C., et al, July 1989.
2. Honeywell Technical Solutions, Inc., Mission Operations and Mission Services, MOMS-FD-UG-0208, *Global Positioning System (GPS) Enhanced Onboard Navigation System (GEONS) System Description and Users Guide*, Version 2, Release 2.4, prepared by Anne Long, and Dominic Leung, August 31, 2005.
3. Honeywell Technical Solutions, Inc., Mission Operations and Mission Services, MOMS-FD-UG-0043, *User's Guide and Mathematical Specifications for the Measurement Data Simulation Program*, Update 4, Revision 1, prepared by Dominic Leung, April 18, 2005.

4. Bamford, B., Winternitz, L., Moreau, M., "Real-Time Geostationary Orbit Determination Using the Navigator GPS Receiver," 2005 Flight Mechanics Symposium, Greenbelt, MD, Oct 18-20, 2005
5. Moreau, M., Naasz, B., Leitner, J., Carpenter, R., and Gaylor, D., "Hardware in-the-Loop Demonstration of Real-Time Orbit Determination in High Earth Orbits," Institute of Navigation NTM 2005, January 2005.
6. Winternitz, L., Moreau, M., Boegner, G., and Sirotzky, S., "Navigator GPS Receiver for Fast Acquisition andWeak Signal Space Applications," Proceedings of the Insitute of Navigation GNSS 2004 Conference, September 2004.
7. Moreau, M., Alxerad., P., Garrison, J., Wennersten, M., and Long, A., "Test Results of the PiVoT Receiver in High Earth Orbits using a GSS GPS Simulator," Proceedings of the Institute of Navigation GPS 2001 Conference, September 2001.
8. Holt, G., Lightsey, E. G., Montenbruck O., "Benchmark Testing for Spaceborne Global Positioning System Receivers", AIAA Guidance, Navigation and Control Conference, Aug 11-14, 2003, Austin Texas.
9. Lyndon B. Johnson Space Center, JSC-25857, "Range Bias Models for GPS Navigation Filters", B. Lear, June 1993.
10. Brown, R. G., and Hwang, P.Y.C., *Introduction to Random Signals and Applied Kalman Filtering*, Third Ed., John Wiley and Sons: New York, 1997.
11. Taylor, Jack, Barnes, Eric, GPS Current Signal-in-Space Navigation Performance, ION National Technical Meeting, San Diego, CA, January, 2005.
12. Czopek, F., "Description and Performance of the GPS Block I and II L-Band Antenna and Link Budget," Proceedings of the Institute of Navigation GPS 93 Conference, 1993.

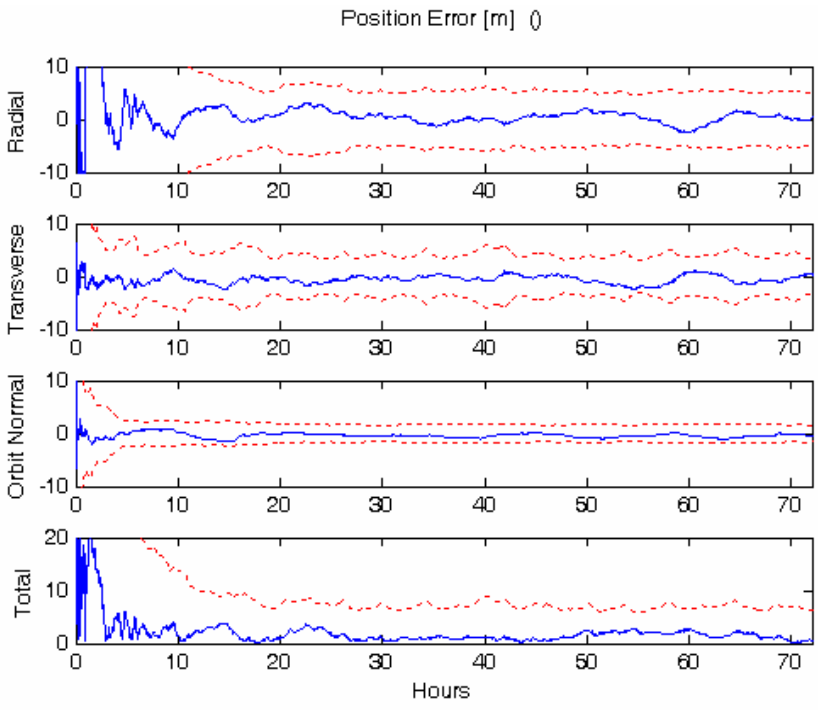

Figure 1 - GEONS position errors from baseline hardware test data.

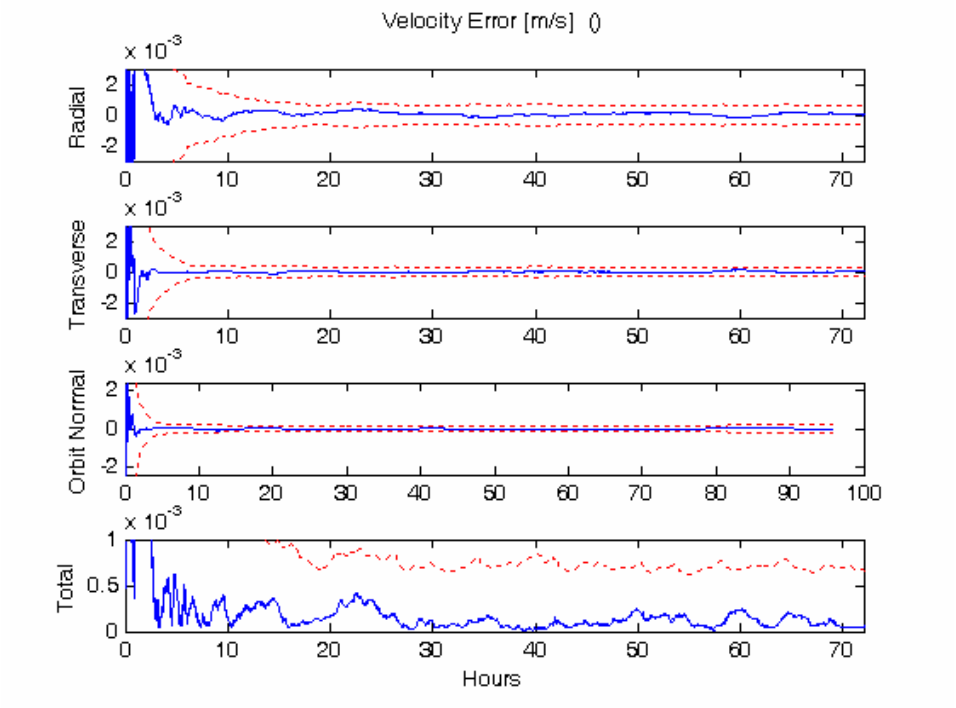

Figure 2 - GEONS velocity errors from baseline hardware test data.

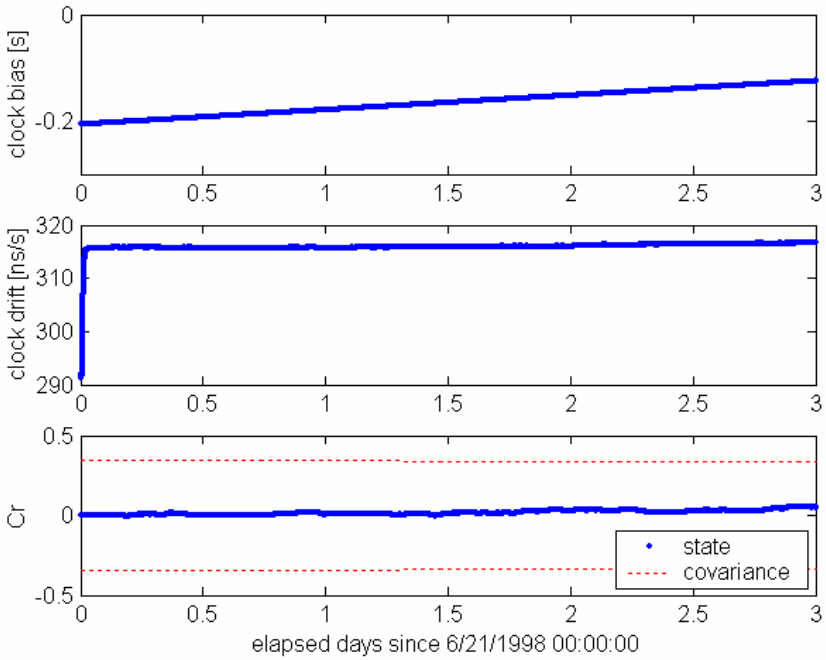

Figure 3 - Other GEONS state estimates from baseline hardware test data.

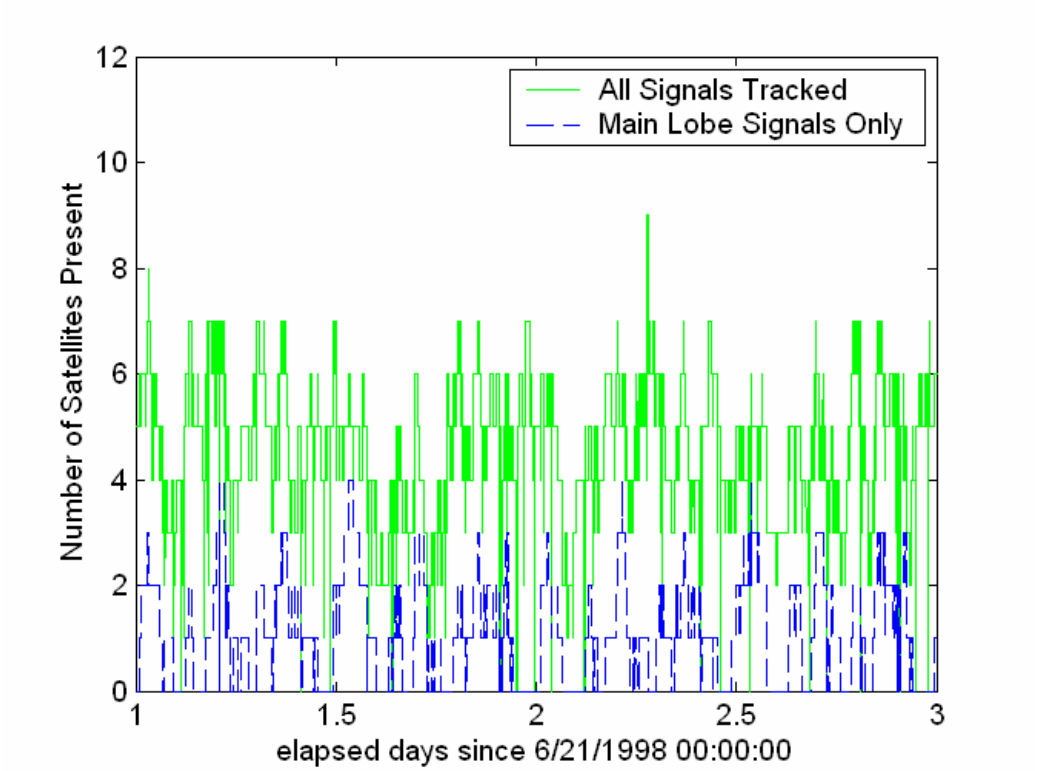

Figure 4 - Number of available GPS signals in hardware test data with and without side lobes.

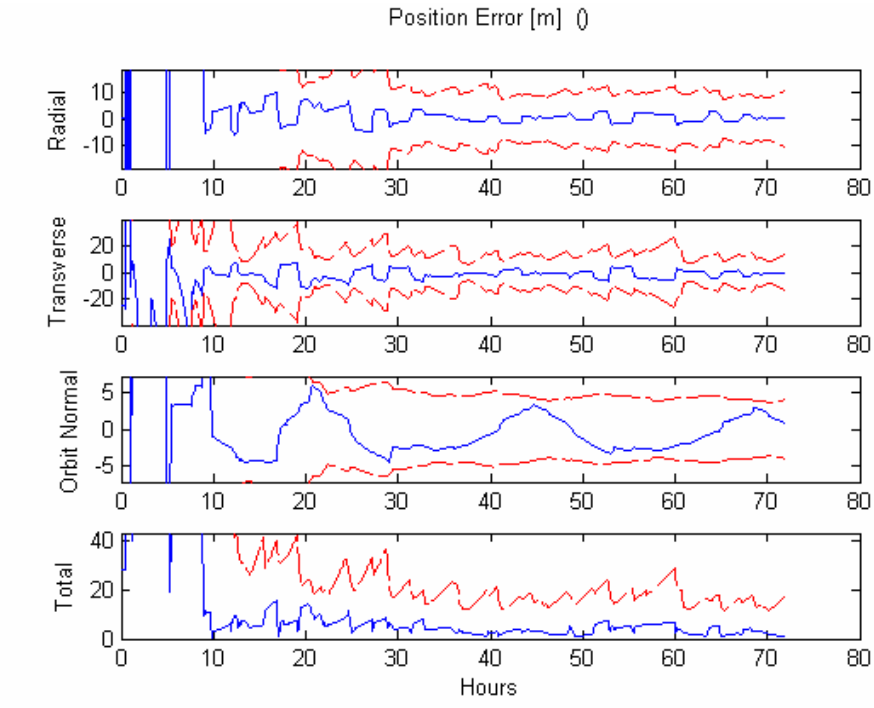

Figure 5 - GEONS position errors from hardware test without side lobes.

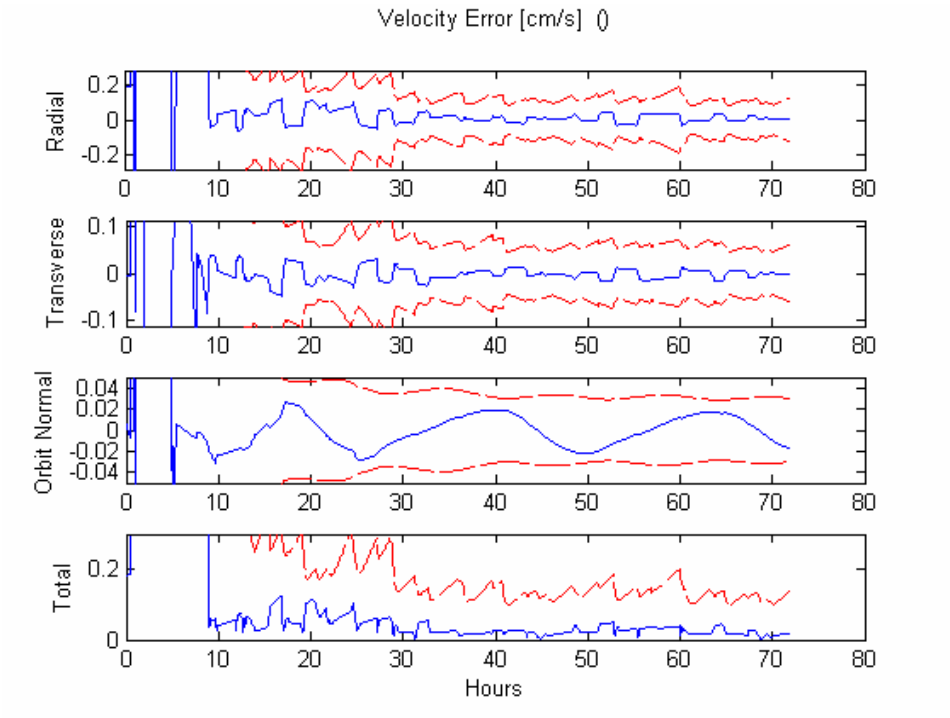

Figure 6 - GEONS velocity errors from hardware test without side lobes.

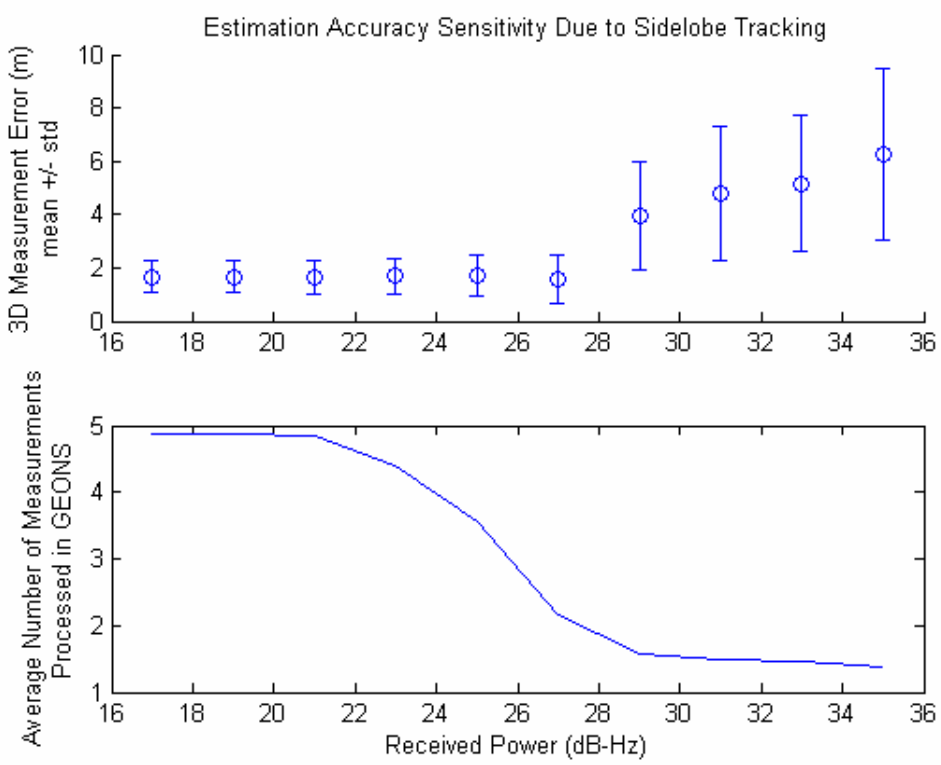

Figure 7 - Sensitivity to receiver acquisition/tracking threshold

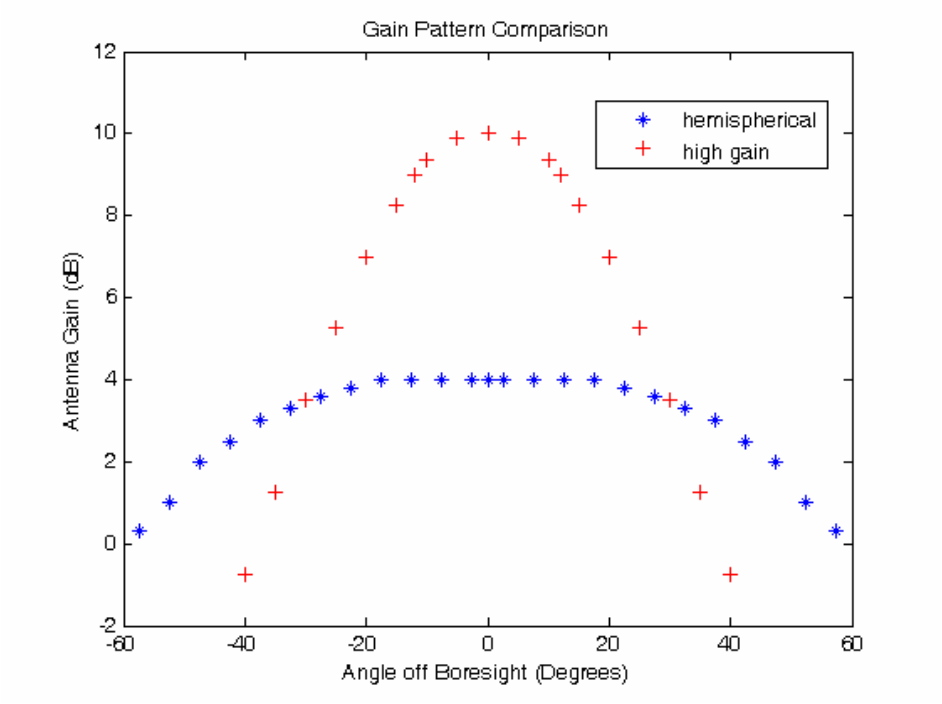

Figure 8 - High Gain and Hemispherical Gain Pattern Comparison

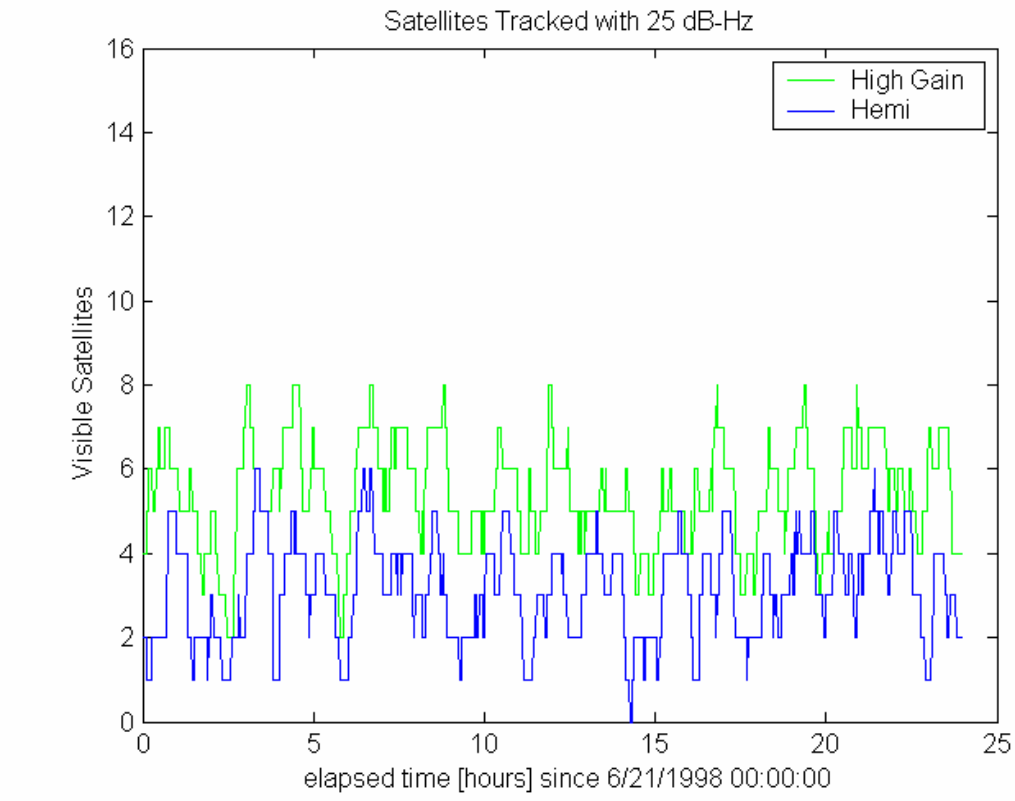

Figure 9 - Tracking Results for High Gain and Hemispherical Antennas

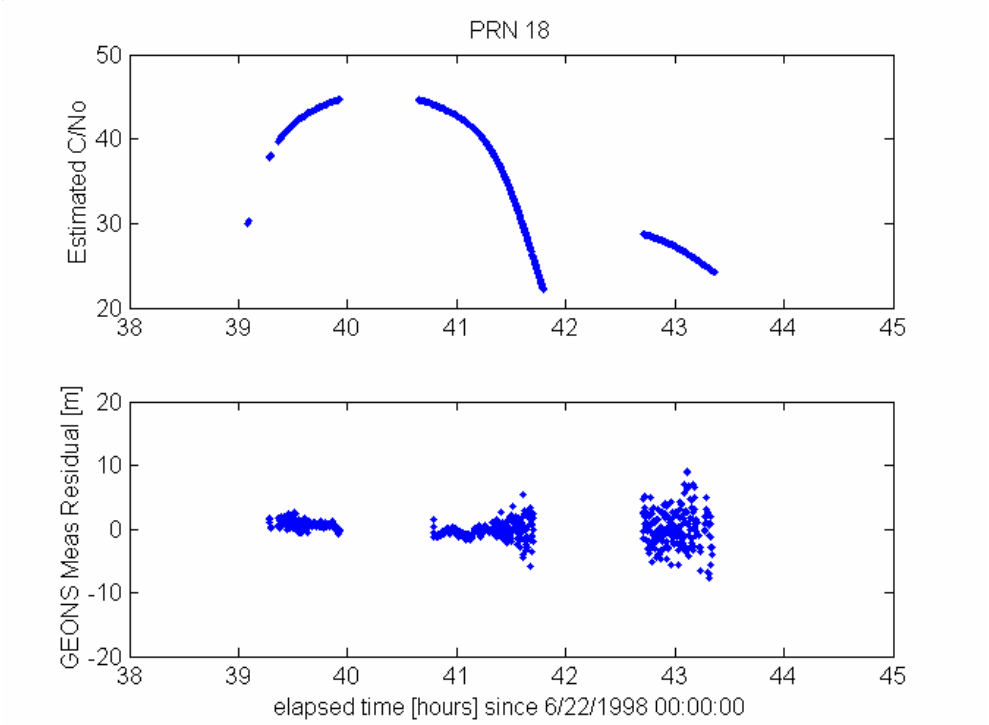

Figure 10 - Variation in Receiver Measurement Noise with C/No

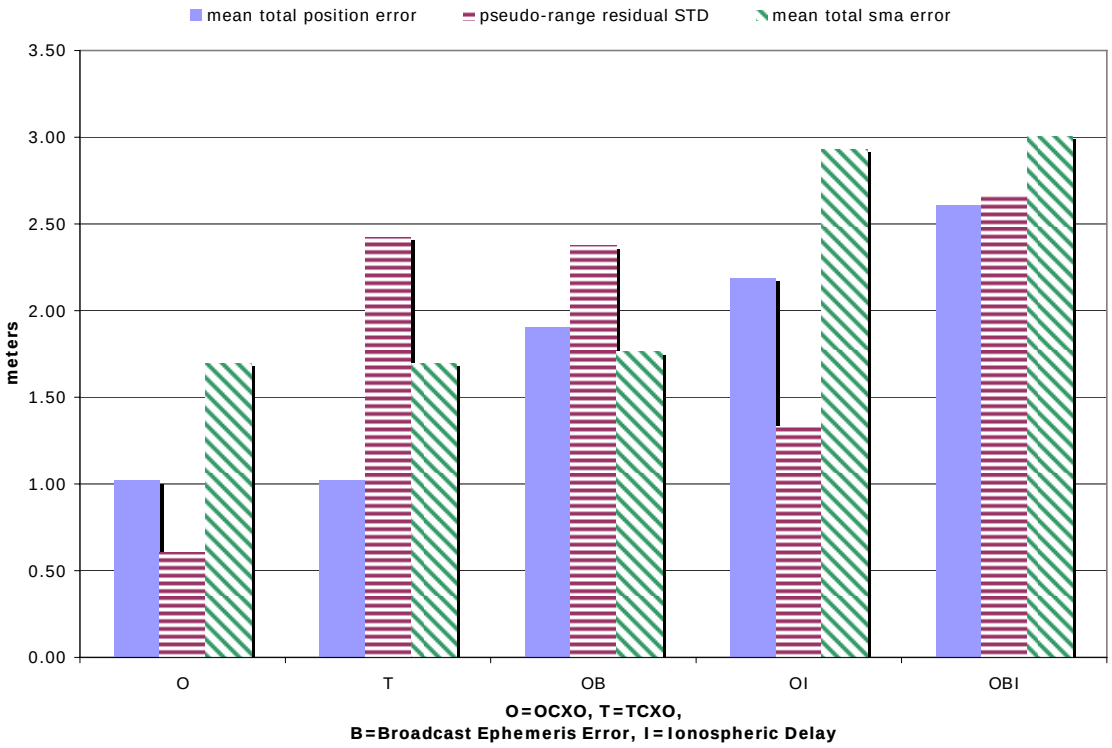

Figure 11 - Software Only (DATSIM) Simulation Results